

We are IntechOpen, the world's leading publisher of Open Access books Built by scientists, for scientists

6,900

Open access books available

185,000

International authors and editors

200M

Downloads

154

Countries delivered to

TOP 1%

most cited scientists

12.2%

Contributors from top 500 universities



WEB OF SCIENCE™

Selection of our books indexed in the Book Citation Index
in Web of Science™ Core Collection (BKCI)

Interested in publishing with us?
Contact book.department@intechopen.com

Numbers displayed above are based on latest data collected.

For more information visit www.intechopen.com



The Relationship between the Collapsing Cavitation Bubble and Its Microjet near a Rigid Wall under an Ultrasound Field

Ce Guo

Additional information is available at the end of the chapter

<http://dx.doi.org/10.5772/intechopen.79129>

Abstract

Cavitation bubble collapse and its produced microjet on a solid wall are very important for the application of ultrasound. However, the prediction and control of microjets have been a very challenging work due to the complicated mechanisms of the collapsing of cavitation bubbles under the ultrasonic field. In order to determine the interaction of the microjet with the key parameters that influence the acoustic cavitation, the dynamics of bubble growth and collapse near a rigid boundary in water are investigated. Numerical simulations of the motion characteristics and collapsed velocities of a bubble near a rigid boundary and a free boundary have been performed. Compared with the free boundary, the rigid boundary has an inhibition effect for ultrasonic cavitation. The velocity of the bubble collapse under the rigid boundary is decreased as the increase of the initial bubble radius and ultrasonic frequency and rises with the increase of the distance from the bubble to the solid wall. There is the optimal acoustic pressure at which ultrasonic cavitation effect near the rigid boundary is most violent. The relationship between the velocity of the bubble collapse and its microjet near a rigid boundary is finally described.

Keywords: ultrasound field, cavitation, bubble, microjet, rigid wall

1. Introduction

The dynamical behavior of the bubble near a solid wall has crucial and practical significance for exploring the industrial application of ultrasonic cavitation. In 1966, Benjamin and Ellis [1] found out that it may lead to a high-speed microjet impinging on a solid wall through the bubble when the pressure on the upper and lower wall of the bubble near a rigid wall was

uneven by the experiment for the first time. Brujan [2] measured the microjet released by the bubble collapse on a solid wall in water utilizing high-speed photography. It was shown that an ultrasonic wave with a frequency of 3.24 MHz has the capacity to generate a microjet of $80\text{--}130 \text{ m}\cdot\text{s}^{-1}$ when bubble's maximum radius is $150 \mu\text{m}$. In addition, Brujan and Ikeda [3] demonstrated that the impact intensity of the microjet can be up to $1.3 \pm 0.3 \text{ GP}$ by capturing the bubble with a radius of $68 \mu\text{m}$ near a solid wall. However, not all bubbles near a solid wall can produce high-speed and large intensity microjets. Vignoli [4] proposed that the microjet would appear only if the velocity of the bubble collapse is higher than or even higher than that of an acoustic wave propagating in a liquid.

The effect of microjets produced by cavitation bubbles under an ultrasound field is widely applied in ultrasonic medicine, ultrasonic chemistry, ultrasonic cleaning [5, 6] and so on. In recent years, the study of cavitation and cavitation erosion near a solid wall has also highly attracted in the field of ultrasonic vibration machining [7, 8]. On the one hand, the oscillating and collapsing bubble generated by ultrasonic cavitation can be used to clean the machining region. On the other hand, the microjet released by the bubble collapse near a solid wall can cause plastic deformation or even brittle fracture on the surface material. Nevertheless, cavitation mechanisms have not been revealed yet due to the complex relationship between the collapsing cavitation bubble and its microjet near a solid wall.

Vibration and collapse mechanisms of the cavitation bubble under the ultrasonic field can be described by motion equations of the bubble. Many scholars studied motion equations of the bubble under the ultrasonic field, some well-known models such as Rayleigh-Plesset equation [9], Gilmore equation [10], Keller-Miksis equation [11], and so on. Although these models are relatively reasonable to explore the dynamical behaviors of the cavitation bubble, they do not consider the action of a solid wall universally. It is certain to simplify calculation if ignoring the effect of a solid wall in analysis of the bubble motion inside a free boundary. However, due to the fact that there are always particle impurities and different types of structural walls in the actual liquid, theoretical models of the cavitation bubble are quite different from the actual environment. Thus, Doinikov [12] deduced a bubble model near a solid wall while exploring coated micro bubbles moving in the blood vessel in 2009. It took the wall thickness of the bubble into account and led to widespread application of ultrasound contrast agents [13, 14]. On the basis, the resonance frequency and vibration displacement of the bubble near a solid wall under an ultrasound field were derived by Qin [15]. It is noted that the solid wall can reduce the resonance frequency and increase the motion damping of the bubble. In order to deeply understand the motion and collapse characteristics of the bubble near a solid wall, the prediction and control strategies of microjets should be discussed theoretically.

In the research, based on the equation of the two bubbles under an ultrasonic field, a model for describing the growth and collapse of the bubble near the solid wall is established. The key parameters that affect the acoustic cavitation, the dynamics of bubble growth and collapse near the solid wall are discussed. The interaction of key parameters with the microjet is finally investigated in detail.

2. Theoretical model

2.1. Dynamical models of the bubble near a rigid wall under an ultrasonic field

Refraction and reflection of acoustic waves will occur during the propagation of an ultrasonic field when it encounters rigid interfaces, for instance, planes, cylinders, or spheres. In the research, the physical process of ultrasound coming into contact with a rigid wall is assumed as total reflection, and the rigid wall is regarded as infinite. In order to reveal the influence of the rigid wall on the bubble motion, the two-bubble motion model of a free boundary under an ultrasound field is introduced at first. The model has assumptions as follows: (1) the bubble maintains a spherical shape during the process of expansion and contraction; (2) the radial motion of the bubble is taken into account, but the translational motion of the bubble is neglected; (3) the viscosity of the liquid, the surface tension, the vapor pressure, and the slight compressibility of the liquid are included; (4) the interaction between adjacent bubbles is also in view; and (5) heat exchange of the liquid, phase transitions of water vapor, gas mass exchange, and chemical reactions inside the bubble are not considered. Then, derived from the Doinikov equation, the dynamical model of two bubbles can be presented as follows [16]:

$$R_i \ddot{R}_i + \frac{3}{2} \dot{R}_i^2 + \frac{1}{D} \frac{d(\dot{R}_j^2 \dot{R}_j)}{dt} = \frac{1}{\rho} \left(p_{gi} + p_v - \frac{2\sigma}{R_i} - 4\eta \frac{\dot{R}_i}{R_i} - p_0 + p_a \sin 2\pi ft \right) + \frac{R_i}{\rho c} \frac{d}{dt} (p_{gi} + p_a \sin 2\pi ft) \quad (1)$$

where the subscript i and j , respectively, represent two different bubbles, R_i is the radius of the bubble i at any time, \cdot indicates the derivative of time, D is the distance between two bubbles, p_{gi} is the gas pressure within the bubble i , p_v is the saturated vapor pressure inside the bubble, ρ is the density of the liquid, σ is the surface tension coefficient of the liquid, η is the viscosity coefficient of the liquid, c is the speed of sound in the liquid, p_0 is the hydrostatic pressure of the liquid, p_a is the acoustic amplitude and f is the ultrasonic frequency.

In the research, the stage of the bubble collapse is the main focus of attention. Due to the fact that the bubble cannot be compressed indefinitely, the procedure of the gas changing inside the bubble is approximately treated as an adiabatic process. Then, the van der Waals gas is introduced to describe the bubble gas in the bubble i near a solid wall. The pressure p_{gi} is described as follows [17]:

$$p_{gi} = \left(p_0 + \frac{2\sigma}{R_{0i}} - p_v \right) \left(\frac{R_{0i}^3 - h_i^3}{R_i^3 - h_i^3} \right)^\gamma \quad (2)$$

where R_{0i} is the initial radius of the bubble i , h_i is the van der Waals radius of the bubble i (for air, $R_{10}/h_i = 8.54$), γ is the multiparty index.

Thus, the bubble near the rigid wall is driven by the fluid pressure in the radial motion, and it can be affected by the action of the incident and reflected ultrasonic wave in particular. The reflection of ultrasonic wave is produced by the incident ultrasonic waves reflecting on the rigid wall. According to the principle of the mirror image, the action behavior of the bubble under the reflected wave near a rigid wall can be seen as that of a virtual mirror bubble under the incident wave. As a result, the motion of the bubble near a rigid wall can be regarded as a special case of the two bubbles system which consists of a bubble and its mirror image.

The coordinate system of the bubble near a rigid wall is established as shown in **Figure 1**, where O_1 and O_2 are the center coordinate of the bubble and its mirrored bubble, l is the distance between the center of the bubble and the rigid wall. There is the symmetric geometric relation of the bubble and the mirrored bubble in nature, that is $D = 2l$. Therefore, ignoring the initial phase effect of the sound wave, the dynamical model of bubbles near a rigid wall under an ultrasonic field can be obtained as follows:

$$R\ddot{R} + \frac{3}{2}\dot{R}^2 + \frac{1}{2l}\frac{d(\dot{R}^2 R)}{dt} = \frac{1}{\rho}\left(p_g + p_v - \frac{2\sigma}{R} - 4\eta\frac{\dot{R}}{R} - p_0 + p_a \sin 2\pi ft\right) + \frac{R}{\rho c}\frac{d}{dt}(p_g + p_a \sin 2\pi ft) \quad (3)$$

Compared with the Doinikov model, Eq. (3) corrects the gas pressure inside the bubble p_g and considers the weak compressibility in a liquid which can be seen in the second term on the right side of Eq. (3). In addition, the influence of the rigid wall on the bubble motion is especially included, which can satisfy the study of the bubble motion near the rigid wall.

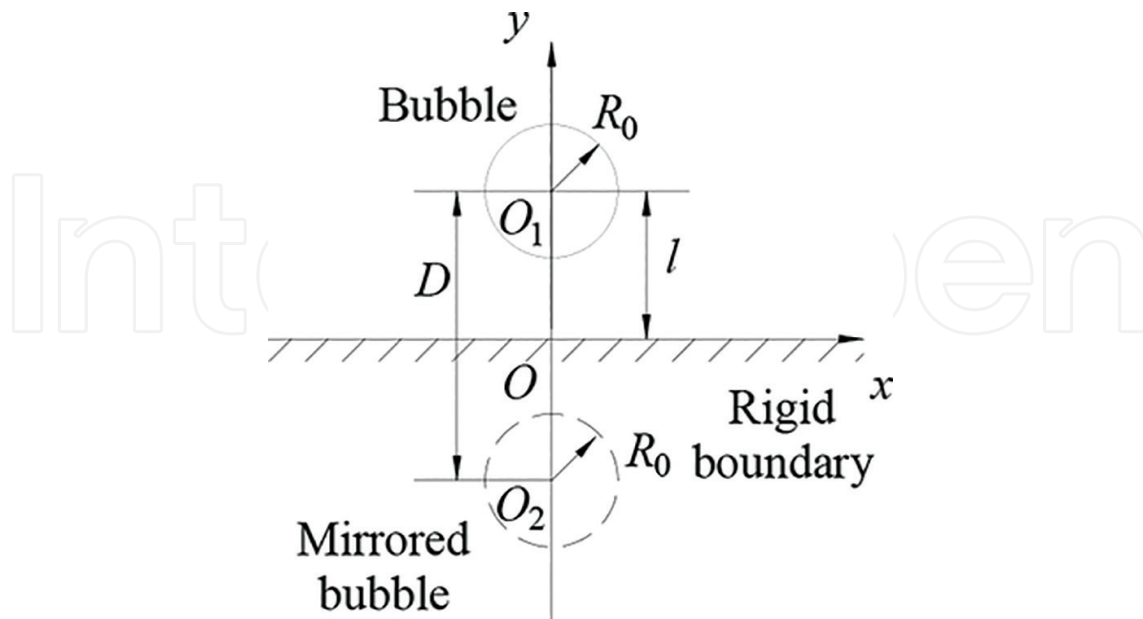


Figure 1. Coordinate system of a bubble near a rigid wall.

2.2. Relationship between the velocity of the bubble collapse and microjet

It is demonstrated that the microjet is caused by the uneven variation of the bubble wall near a solid wall. Since the bubble model is assumed as doing a spherical motion, we focus on the relationship between the velocity of the bubble collapse and microjet, in which the bubble is compressed to a minimum value. The nonspherical variation on the bubble wall is not included in the scope of this study. Thus, a simplified equation describing the bubble collapse is introduced as follows [18]:

$$v_{\text{collapse}} \approx \frac{2}{3} \frac{p_{\infty} - p_v}{\rho} \left(\frac{R_{\max}^3}{R_0^3} - 1 \right) \quad (4)$$

where p_{∞} is the liquid pressure at infinity distance around the bubble, R_{\max} is the maximum radius of the bubble.

Blake and Gibson [19] indicated that the formation of the microjet is closely related to the bubble radius and the distance from the bubble to the solid wall through experiments. Ohl [20] and Tzanakis [21] used high-speed photography to record the relationship between the variation of the bubble wall and microjets near a solid wall. The results illustrated that the microjet produced by the bubble near the solid wall can be interpreted as the ratio of the maximum value of the bubble expansion to the collapse time of the bubble, which can be expressed approximately as follows:

$$v_{\text{microjet}} \approx \frac{2 R_{\max}}{t_{\text{collapse}}} \quad (5)$$

where t_{collapse} is the collapse time of the bubble. Based on the theory of Rayleigh [22], the collapse time of the bubble can be expressed as:

$$t_{\text{collapse}} \approx 0.915 R_0 \sqrt{\frac{\rho}{p_{\infty} - p_v}} \quad (6)$$

Combining Eqs. (4)–(6), the relationship between the velocity of the bubble collapse and microjet can be expressed as follows:

$$v_{\text{microjet}} = 2.677 \sqrt{\frac{v_{\text{collapse}} R_{\max}^2 R_0}{R_{\max}^3 - R_0^3}} \quad (7)$$

2.3. Numerical simulation and initial conditions

The initial conditions for the simulation are when $t = 0$, $R = R_0$, $dR/dt = 0$. It is assumed that the liquid temperature is 20° , and the main physical parameters are as follows: $\rho = 1.0 \times 10^3 \text{ kg}\cdot\text{m}^{-3}$, $\sigma = 7.2 \times 10^{-2} \text{ N}\cdot\text{m}^{-1}$, $p_v = 2.33 \times 10^3 \text{ Pa}$, $c = 1.5 \times 10^3 \text{ m}\cdot\text{s}^{-1}$, $\eta = 1.0 \times 10^{-3} \text{ Pa}\cdot\text{s}$, $\gamma = 4/3$. Therefore, the differential equation of Eqs. (2) and (3) for describing the dynamics of the bubble near a rigid wall can be calculated numerically by the Runge-Kutta fourth-order method. Taking

Eqs. (2), (3), and (5) into Eq. (7), the relationship between the velocity of the bubble collapse and microjet can be further obtained.

3. Results and discussion

3.1. Comparison of the bubble motion near a free boundary and a rigid boundary under an ultrasonic field

Figure 2 shows the motion characteristics of a bubble near a free boundary and a rigid boundary under an ultrasonic field in five sound cycles, for ultrasonic frequency of 20 kHz and acoustic amplitude of 0.2 MPa. The initial bubble radius is 10 μm , and the dimensionless distance from the bubble to the rigid boundary (l/R_0) is set to 1. The bubble motion near a rigid boundary is described by Eq. (3), and the bubble motion with a free boundary can be further obtained by ignoring the effect of the solid wall of Eq. (3), that is without the left third item in Eq. (3).

Figure 2(a) displays the variation of the bubble radius versus time. It can be seen that even though the bubble undergoes the dynamic process of growth, expansion, compression, collapse and rebound under the action of five sound cycles, there are obvious differences of the bubble radius in the two cases. Compared with the case under the free boundary, the bubble near the rigid boundary has a lower maximum radius and a longer collapse time. It illustrates that the process of bubble expansion and compression becomes slower because of the existence of the rigid boundary, that is, the rigid boundary plays a part in suppressing the bubble motion.

Figure 2(b) shows the variation of the bubble velocity versus time. As can be seen, the closer the bubble minimum radius, the greater is the bubble velocity. When the bubble radius is compressed to the minimum radius, the maximum velocity of the bubble can be obtained.

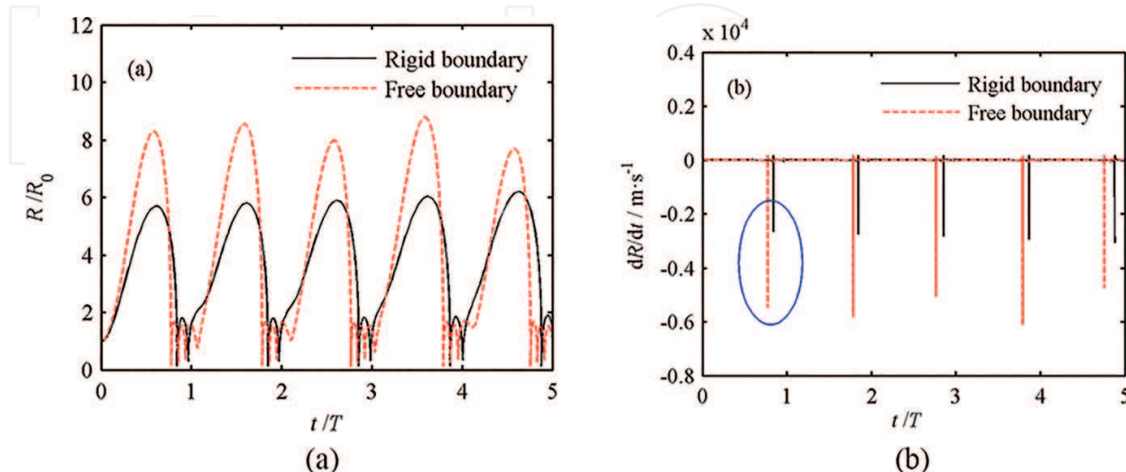


Figure 2. Motion characteristics of a bubble near a rigid boundary and a free boundary under ultrasound field: (a) bubble radius versus time and (b) bubble velocity versus time.

There is the damping of the sound wave in the liquid, and the oscillation of the bubble will become weaker and weaker, and thus the first sound cycle is taken an example to describe the bubble collapse approximately. Furthermore, for the free boundary, the bubble radius can be compressed to 0.1408 of the initial radius extremely, and the maximum velocity of the bubble can be up to $5422 \text{ m}\cdot\text{s}^{-1}$. However, for the rigid boundary, the bubble radius can merely be compressed to 0.1453 of the initial radius and the bubble velocity is $2661 \text{ m}\cdot\text{s}^{-1}$. Thus, compared with the free boundary, the compression ratio of the bubble under the rigid boundary is lower and the velocity of the bubble collapse is smaller. It also indicates that the rigid boundary has an inhibition effect for the bubble collapse.

3.2. Effects of parameters on the velocity of the bubble collapse

The collapse and rebound of the bubble near the rigid wall are closely related to the effects of microjets and shock waves of ultrasonic cavitation. To further study the effects of bubble collapse near the solid wall, the main parameters affecting the bubble collapse will be analyzed in the following aspects. In view of that, the theoretical and experimental research about acoustic cavitation are usually concerned about the size of the velocity of the bubble collapse [23], and the maximum value of the bubble velocity in an acoustic cycle is selected to record the velocity of the bubble collapse (v_{collapse}).

3.2.1. Effect of the bubble initial radius

Figure 3 shows the velocity of the bubble collapse versus the initial bubble radius for the ultrasonic frequency of 20 kHz, acoustic amplitude of 0.2 MPa and the dimensionless distance from the bubble to the rigid boundary of 1, for various initial bubble radius (10–100 μm). The

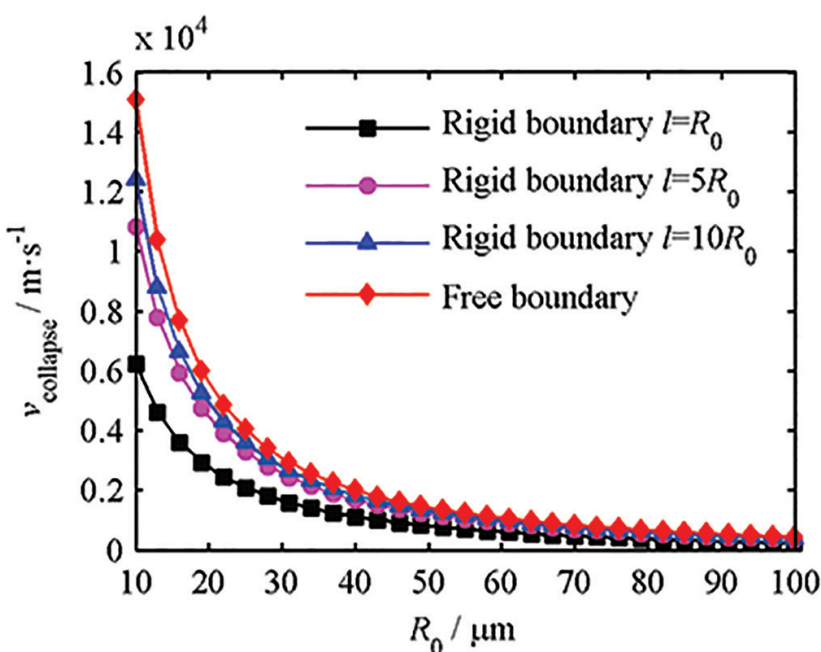


Figure 3. Velocity of the bubble collapse versus the initial bubble radius.

reason for the selection of that range of the bubble initial radius is that it is a common value for discussing cavitation and cavitation erosion [24]. As can be seen, the smaller the initial bubble radius, the higher is the velocity of the bubble collapse. With the increase of the initial bubble radius, the velocity of the bubble collapse decreases rapidly, which means the intensity of ultrasonic cavitation is weakened. This is mainly because the initial radius of the bubble used in the research is smaller than the resonance radius of the bubble (according to Minneart's theory, an ultrasonic wave with a frequency of 20 kHz has a resonance radius of several hundred micrometers [25]). Thus, for a bubble with a larger initial radius, it will begin to compress before it grows to the maximum. As a result, the expansion of the bubble is weakened, and the collapse time is prolonged, which results in the decrease of the velocity of the bubble collapse. For the same bubble initial radius, the velocity of the bubble collapse under the case of the rigid boundary is lower than that of the free boundary. In addition, in **Figure 3**, with the increase of the dimensionless distance from the bubble to the rigid boundary, the velocity of the bubble collapse gradually increases. The farther the distance from the bubble to the rigid boundary, the closer is the velocity of the bubble collapse under the rigid boundary to it under the free boundary. It indicates that compared with the free boundary, the rigid boundary suppresses the process of the bubble collapse among the discussed initial bubble radii.

3.2.2. Effect of the distance from the bubble to the solid wall

Figure 4 shows the velocity of the bubble collapse versus the distance from the bubble to the solid wall for the ultrasonic frequency of 20 kHz, acoustic amplitude of 0.2 MPa and the initial bubble radius of 20 μm , for the dimensionless distance from the bubble to the rigid boundary ($1R_0$ – $51R_0$). It can be seen from **Figure 4**, the velocity of the bubble collapse under the free boundary can be up to $5569 \text{ m}\cdot\text{s}^{-1}$, and it is not related to the distance from the bubble to the solid wall. However, for the bubble near the rigid boundary, the distance from the bubble to the solid wall has a significant effect on the velocity of the bubble collapse. When the dimensionless distance between the bubble and the solid wall is relatively small, for instance, the bubble is just close to the solid wall, the velocity of the bubble collapse is $2756 \text{ m}\cdot\text{s}^{-1}$. With the increase of the distance from bubble to solid wall, the inhibitory action of the solid wall on the bubble motion is diminished and thus the velocity of the bubble collapse increases. Moreover, the greater the distance between the bubble and the solid wall, the slower is the increasing of the velocity of the bubble collapse. When the dimensionless distance from the bubble to the rigid boundary is 51, the velocity of the bubble collapse is $5422 \text{ m}\cdot\text{s}^{-1}$ which is very close to that of $5569 \text{ m}\cdot\text{s}^{-1}$ under the free boundary. It indicates that the farther the distance from the bubble to the solid wall, the smaller is the influence of the solid wall on the bubble. When the distance of the bubble away from the solid wall is up to a certain value, the effect of the solid wall on the bubble is almost negligible. In the situation, the bubble motion near the rigid boundary can be regarded as that under the free boundary.

3.2.3. Effect of acoustic pressure amplitude

Figure 5 shows the velocity of the bubble collapse versus the acoustic pressure amplitude for the ultrasonic frequency of 20 kHz, the initial bubble radius of 20 μm and the dimensionless

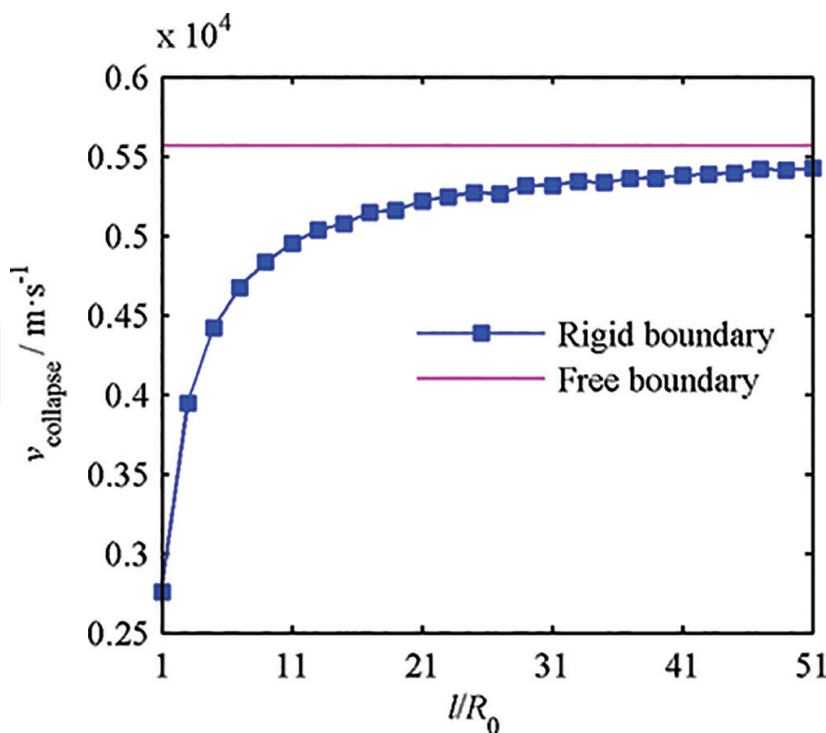


Figure 4. Velocity of the bubble collapse versus the distance from the bubble to the solid wall.

distance from the bubble to the rigid boundary of 1, for various acoustic pressure amplitude ($0p_0 - 5p_0$). As can be seen from **Figure 5**, the acoustic pressure amplitude has a special influence on the velocity of the bubble collapse. When the acoustic pressure amplitude is very low, such as $p_a \leq 1p_0$, the velocity of the bubble collapse is almost close to zero for both free and rigid boundary. It is owing to the fact that the acoustic pressure amplitude is so lower that it is still unable to overcome the hydrostatic pressure of the liquid. Thus, in the case, the liquid has not yet caused cavitation. With the increase of the acoustic pressure amplitude, the velocity of the bubble collapse under the rigid boundary is different from the case under the free boundary. For the free boundary, with the increase of the acoustic pressure amplitude, such as $p_a > 1p_0$, the velocity of the bubble collapse increases nearly in a linear manner. It illustrates that for a bubble in a free liquid, the increase of the acoustic pressure amplitude can significantly improve the severity of cavitation. Compared with the case under the free boundary, on the one hand, the velocity of the bubble collapse under the rigid boundary is lower because of the inhibitive action of the rigid boundary. On the other hand, the variation of the velocity of the bubble collapse under the rigid boundary is more special and complex. When $p_a > 1p_0$, with the increase of the acoustic pressure amplitude, the velocity of the bubble collapse presents the trend of increasing first and then decreasing. In addition, for the bubble near the rigid wall, it is noted that there is an optimal value of the acoustic pressure amplitude. Under the optimal value, the bubble collapse can be maximized. For instance, when the bubble is just close to the solid wall, that is $l = R_0$, the velocity of the bubble collapse can be up to the maximum value at the acoustic pressure amplitude of 3.5 p_0 and it demonstrates there is the strongest cavitation effect. With the increase of the distance from the bubble to the solid wall, the optimal value of the acoustic pressure amplitude will gradually increase. When the bubble is far enough from the rigid boundary, the bubble motion

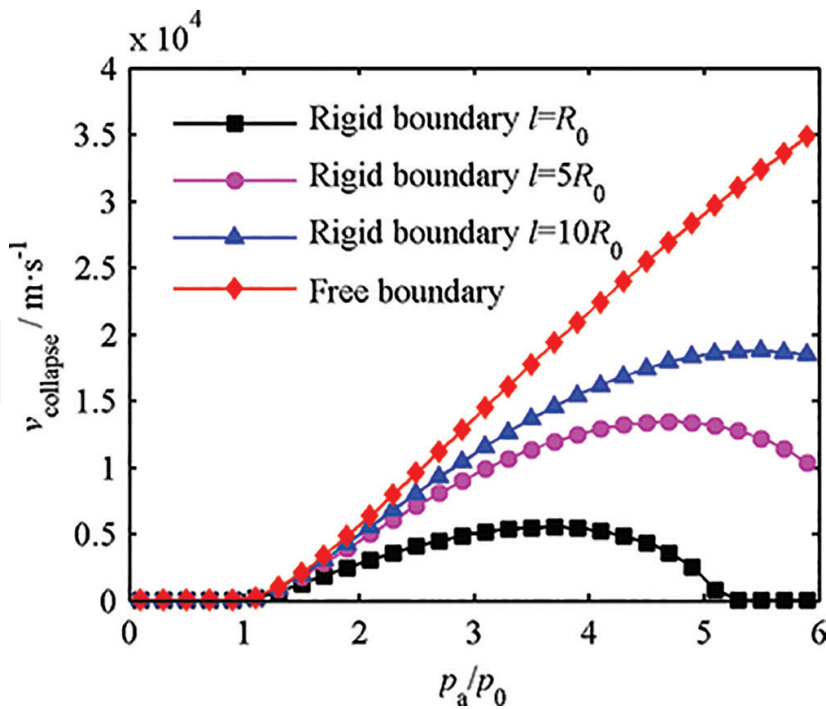


Figure 5. Velocity of the bubble collapse versus the acoustic pressure amplitude.

and collapse are equal to that under the free boundary, and then the optimal value of the acoustic pressure amplitude is not found easily.

3.2.4. Effect of ultrasound frequency

Figure 6 shows the velocity of the bubble collapse versus the ultrasonic frequency for the acoustic pressure amplitude of 0.2 MPa, the initial bubble radius of 20 μm and the dimensionless distance from the bubble to the rigid boundary of 1, for various ultrasonic frequency (18–30 kHz). As can be seen from **Figure 6**, when the ultrasonic frequency is low, the velocity of the bubble collapse is high. As the ultrasonic frequency increases, the velocity of the bubble collapse gradually decreases. It means that a weaker effect of the cavitation will be obtained with the increase of the ultrasonic frequency. It is mainly due to the fact that with the increase of ultrasonic frequency, the cycles of the bubble expansion and compression are getting faster and faster. Thus, the bubble may not have enough time to grow to produce the cavitation effect or the bubble may not be compressed enough to collapse. These may result in reducing the growth and collapse of the bubble and further reducing acoustic cavitation effect. Especially for the higher-frequency ultrasound, the bubble does not have enough time to store the ultrasonic energy and begins to collapse. Therefore, when the ultrasonic frequency is increasing, the velocity of the bubble collapse will continue to decrease, and eventually it will tend to be stable. It can also be found in **Figure 6**, the velocity of the bubble collapse under the rigid boundary is lower than that under the free boundary, at the same ultrasonic frequency. When the ultrasonic frequency varies from 18 to 30 kHz, the velocity of the bubble collapse is reduced by 48.84 and 53.94% under the rigid and free boundary, respectively. Moreover, as the increase of the distance from the bubble to the solid wall, the velocity of the bubble

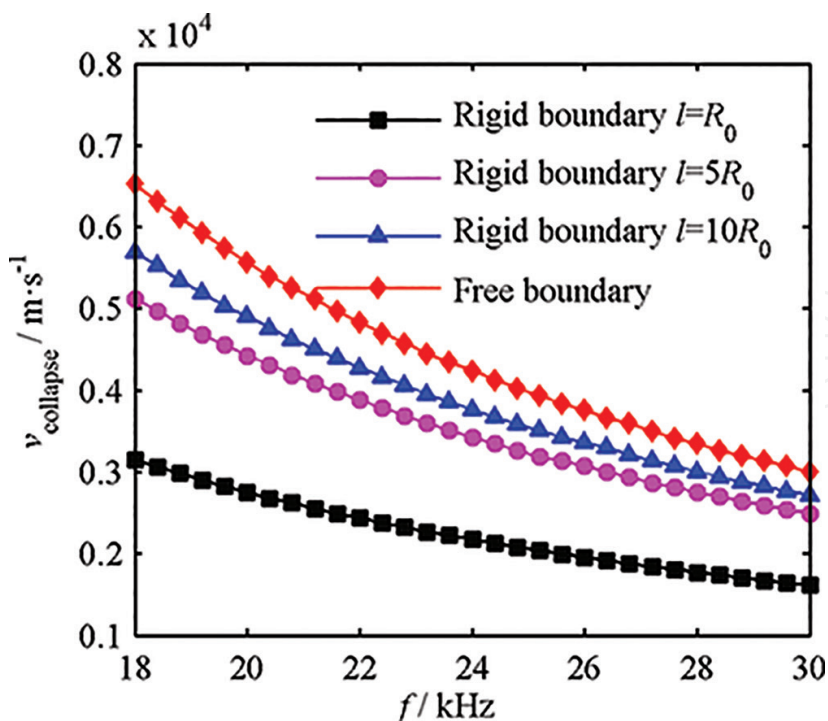


Figure 6. Velocity of the bubble collapse versus the ultrasonic frequency.

collapse is getting higher. It presents that from the control point of view of the ultrasonic frequency, with the increase of ultrasonic frequency, the bubble under the rigid boundary is more easily to collapse than that under the rigid boundary.

3.3. Relationship between the velocity of the bubble collapse and microjet

Figure 7 shows the relationship between the velocity of the bubble collapse and the microjet under the action of one sound cycle, for the ultrasonic frequency of 20 kHz, the initial radius of the bubble of 20 μm and the dimensionless distance from the bubble to the rigid wall of 1. It can be seen from **Figure 7**, the velocity of the microjet responds to changes in the velocity of the bubble collapse, with the increase of the acoustic pressure amplitude. From the above analysis of **Figure 5**, the velocity of the bubble collapse can be up to the maximum value ($5488 \text{ m} \cdot \text{s}^{-1}$) at the acoustic pressure amplitude of $3.5 p_0$, which is the optimal value of the acoustic pressure amplitude. However, in **Figure 7**, the velocity of the microjet reaches a maximum ($67.9 \text{ m} \cdot \text{s}^{-1}$), corresponding to the acoustic pressure amplitude of $3.1 p_0$, which can be treated as another optimum value of acoustic pressure amplitude to improve the microjet effect. It can be seen that the optimum value of the acoustic pressure amplitude of the microjet is lower than that of the velocity of the bubble collapse. In addition, the dotted line in **Figure 7** represents the position where the velocity of the bubble collapse is $1500 \text{ m} \cdot \text{s}^{-1}$, and the acoustic pressure amplitude is relevant to $1.6 p_0$. When $p_a \leq 1.6 p_0$, the velocity of the bubble collapse is less than the propagation velocity of an ultrasonic wave in water ($1500 \text{ m} \cdot \text{s}^{-1}$), in which there is no microjet appearing near the solid wall. Thus, it can be determined that the analysis for the velocity of the bubble collapse is contributed to seek the optimal value of the microjet and to distinguish the range of the variation of the microjet. Based on the earlier analysis, the velocity

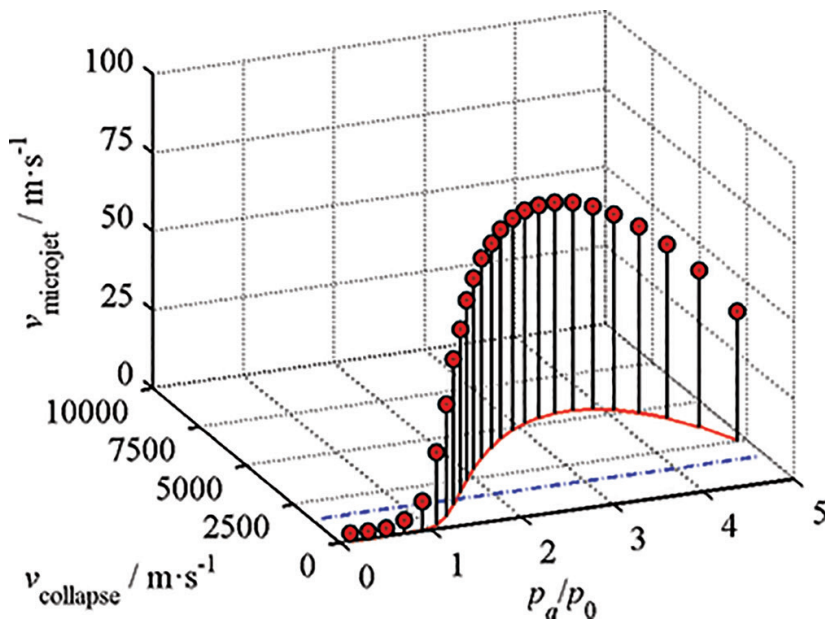


Figure 7. Relationship between the collapse velocity of a bubble and microjet under acoustic pressure.

of the microjet depends on the velocity of the bubble collapse and changes with the velocity of the bubble collapse. Control and utilization of the velocity of the bubble collapse can be used indirectly to achieve the control of the microjet.

Figure 8 shows the relationship between the velocity of the bubble collapse and the microjet under various ultrasonic frequencies. It can be seen that the variation of the velocity of the microjet has the corresponding law to the velocity of the bubble collapse under different ultrasonic frequency. Furthermore, it can be known from Eq. (7) that the velocity of the micro-jet is also directly affected by the radius parameters of the bubble such as R_0 and R_{\max} . Thus, in **Figure 8**, the velocity of the microjet presents a different variation from the velocity of the bubble collapse occasionally, such as a turning point on the curve of the microjet with the ultrasonic frequency of 28 kHz.

At present, many scholars have used the high-speed photography technique to observe and track the ultrasonic cavitation effect and obtain the same variational laws of microjets near the solid wall. However, because of the instability of the bubble collapse near the solid wall of different targets, the accuracy of the measuring instruments and human errors and so on, the quantitative measurement of the velocity of microjets has not been fixed. In order to verify the rationality of the theoretical model, the bubble model and its relationship with the microjet will be examined under different acoustic cavitation test conditions near the rigid wall.

Table 1 shows the velocity comparison between the literature and the model of the microjet. Numbers 1–3 in **Table 1** are the experiment results of the microjet, and Number 4 is the numerical simulation results of the microjet. It can be seen from **Table 1**, at a higher ultrasonic frequency or a larger acoustic amplitude, the error between the model and the literature on the value of the microjet is relatively great, which can be illustrated by numbers 1 and 3. It is because that when the ultrasonic frequency is high or the acoustic amplitude is large,

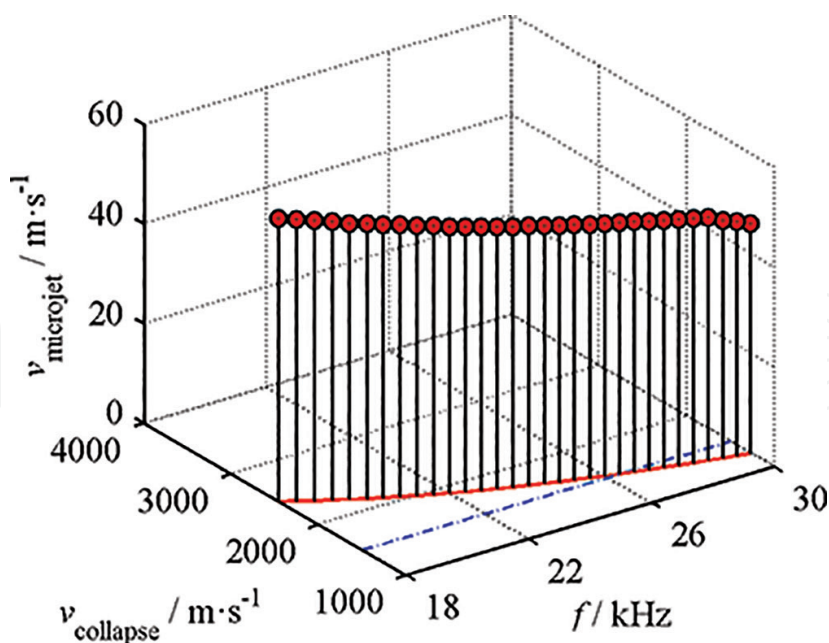


Figure 8. Relationship between the velocity of the bubble collapse and microjet under ultrasonic frequency.

| Number | Microjet/(m·s ⁻¹) | |
|--------|-------------------------------|-------|
| | Literature | Model |
| 1 | 80–130 [2] | 19.98 |
| 2 | 25–30 [4] | 24.57 |
| 3 | 15–20 [24] | 123 |
| 4 | 33.8 [23] | 49.43 |

Table 1. Velocity comparison between the literature and the model of the microjet.

the bubble will oscillate for many sound cycles before it begins to collapse. It leads to the inconvenience of the reasonable selection of initial parameters such as the maximum radius of the bubble and the velocity of the bubble collapse, and thus the instability of the numerical calculation of microjets will increase. However, to sum up, the calculated values of the microjet produced by the ultrasonic cavitation in the research approximately equal to the literature values, and it is to be in the range of an order of magnitude error. Therefore, the bubble model and its relationship with the microjet have certain rationality in the theoretical prediction for the microjet generated by the ultrasonic cavitation under the rigid boundary.

4. Conclusion

In the research, the dynamical model of the bubble near the rigid boundary is established using the principle of the mirror image, and the growth and collapse characteristics of the bubble are

analyzed. The results of numerical analysis illustrate that the bubble under the rigid boundary has a lower maximum radius and a longer collapse time than the bubble under the free boundary, which indicates that the rigid boundary has an inhibition effect for ultrasonic cavitation. The velocity of the bubble collapse decreases with the increase of the initial radius of the bubble, and it rises with the increase of the dimensionless distance from the bubble to the solid wall. Especially when the bubble reaches a certain value away from the solid wall, the bubble motion near the solid boundary can be approximated as the bubble motion under the free boundary. Whatever for the solid boundary and the free boundary, when the acoustic pressure amplitude is less than $1 p_0$, the ultrasonic cavitation cannot form in the liquid. For the free boundary, the velocity of the bubble collapse rises approximately linearly, as the acoustic pressure amplitude is greater than $1 p_0$. However, the velocity of the bubble collapse under the rigid boundary can increase first and then decrease. Thus, the optimal acoustic pressure amplitude can be obtained, at which the velocity of the bubble collapse can be up to maximum and cavitation effect is most violent. In addition, the velocity of the bubble collapse under the free boundary decreases faster than that under the rigid boundary, and then it can decrease as the ultrasonic frequency increases. Based on that, the relationship between the velocity of the bubble collapse and the microjet is established. It can be determined that the analysis for the collapse velocity of the bubble is contributed to seek the optimal value of the microjet and furthermore to achieve the purpose of indirect judgment and control microjets. Moreover, the velocity of the microjet obtained in the research is in the range of tens of micrometers, which is nearly the same magnitude with the experiments measured by Brujan and other scholars. Therefore, it can be considered that the bubble model and its relationship with the microjet have a certain reference value in theory, which provides an implication for further understanding the dynamics of cavitation bubbles on the solid wall induced by the ultrasonic field.

Acknowledgements

The research was primarily supported by the National Natural Science Foundation of China (51275490 and 50975265), the open foundation of Shanxi Key Laboratory of Advanced Manufacturing Technology (XJZZ201601-06) and the school fund of Taiyuan University of Technology (2016QNOZ). I would like to express my gratitude to all those who helped me during the writing of this work. Specially, I would like to express my gratitude to my students Yang Fengyu and Yao Binting, who helped me to revise the English translation.

Appendices and nomenclature

| | |
|-----|------------------------------|
| c | speed of sound in the liquid |
| D | distance between two bubbles |
| f | ultrasonic frequency |

| | |
|-----------------------|--|
| h | van der Waals radius of the bubble |
| l | distance between the center of the bubble and the rigid wall |
| p_a | acoustic pressure amplitude |
| p_g | gas pressure within the bubble |
| p_v | saturated vapor pressure inside the bubble |
| p_0 | hydrostatic pressure of the liquid |
| p_∞ | liquid pressure at infinity distance around the bubble |
| R | radius of the bubble |
| R_{\max} | maximum radius of the bubble |
| R_0 | initial radius of the bubble |
| t_{collapse} | collapse time of the bubble |
| v_{microjet} | velocity of the microjet |
| v_{collapse} | velocity of the bubble collapse |
| i, j | different bubbles |
| γ | multiparty index |
| η | viscosity coefficient of the liquid |
| σ | surface tension coefficient of the liquid |
| ρ | density of the liquid |

Author details

Ce Guo

Address all correspondence to: guoce1027@163.com

College of Mechanical Engineering, Taiyuan University of Technology, Taiyuan, China

References

- [1] Benjamin TB, Ellis AT. The collapse of cavitation bubbles and the pressures thereby produced against solid boundaries. Philosophical Transactions of the Royal Society of London. 1966;260(1110):221-240. DOI: 10.1098/rsta.1966.0046

- [2] Brujan EA, Matsumoto Y. Collapse of micrometer-sized cavitation bubbles near a rigid boundary. *Microfluidics and Nanofluidics*. 2012;13(6):957-966. DOI: 10.1007/s10404-012-1015-6
- [3] Brujan EA, Ikeda T, Matsumoto Y. On the pressure of cavitation bubbles. *Experimental Thermal and Fluid Science*. 2008;32(5):1188-1191. DOI: 10.1016/j.expthermflusci.2008.01.006
- [4] Vignoli LL, ALF DB, RCA T, et al. Modeling the dynamics of single-bubble sonoluminescence. *European Journal of Physics*. 2013;34(3):679-688. DOI: 10.1088/0143-0807/34/3/679
- [5] Dong J, Liu Y, Liang Z, Wang W. Investigation on ultrasound-assisted extraction of salvianolic acid B from *Salvia miltiorrhiza* root. *Ultrasonics Sonochemistry*. 2010;17(1):61-65. DOI: 10.1016/j.ulsonch.2009.05.006
- [6] Merouani S, Hamdaoui O, Rezgui Y, Guemini M. Theoretical procedure for the characterization of acoustic cavitation bubbles. *Acta Acustica United with Acustica*. 2014;100(5):5020-5025. DOI: 10.3813/AAA.918762
- [7] Guo C, Zhu X. Effect of ultrasound on dynamics characteristic of the cavitation bubble in grinding fluids during honing process. *Ultrasonics*. 2017;84:13-24. DOI: 10.1016/j.ultras.2017.09.016
- [8] Guo C, Zhu X, Liu J, Zhang D. Cavitation bubble dynamics induced by hydrodynamic pressure oil film in ultrasonic vibration honing. *Journal of Tribology*. 2018;140:041707. DOI: 10.1115/1.4039409
- [9] Galavani Z, Rezaei-Nasirabad R, Bhattacharai S. On the dynamics of moving single bubble sonoluminescence. *Physics Letters A*. 2010;374(44):4531-4537. DOI: 10.1016/j.physleta.2010.09.017
- [10] Mahdi M, Ebrahimi R, Shams M. Numerical analysis of the effects of radiation heat transfer and ionization energy loss on the cavitation bubble's dynamics. *Physics Letters A*. 2011;375(24):2348-2361. DOI: 10.1016/j.physleta.2011.04.026
- [11] Ida M, Naoe T, Futakawa M. On the effect of microbubble injection on cavitation bubble dynamics in liquid mercury. *Nuclear Instruments and Methods in Physics Research A*. 2009;600(2):367-375. DOI: 10.1016/j.nima.2008.11.124
- [12] Doinikov AA, Aired L, Bouakaz A. Acoustic scattering from a contrast agent microbubble near an elastic wall of finite thickness. *Physics in Medicine and Biology*. 2011;56(21):6951-6967. DOI: 10.1088/0031-9155/56/21/012
- [13] Mettin R, Doinikov AA. Translational instability of a spherical bubble in a standing ultrasound wave. *Applied Acoustics*. 2009;70(10):1330-1339. DOI: 10.1016/j.apacoust.2008.09.016
- [14] Holsteens F, Lippert A, Lechner F, Otto A, et al. Cleaning of semiconductor substrates by controlled cavitation. *Journal of the Acoustical Society of America*. 2008;123(5):3045. DOI: 10.1121/1.2932737

- [15] Qin S, Ferrara KW. The natural frequency of nonlinear oscillation of ultrasound contrast agents in microvessels. *Ultrasound in Medicine and Biology*. 2007;33(7):1140-1148. DOI: 10.1016/j.ultrasmedbio.2006.12.009
- [16] Doinikov AA. Translational motion of two interacting bubbles in a strong acoustic field. *Physical Review E - Statistical, Nonlinear, and Soft Matter Physics*. 2001;64(2):026301. DOI: 10.1103/PhysRevE.64.026301
- [17] Liu B, Cai J, Li F, Huai X. Simulation of heat transfer with the growth and collapse of a cavitation bubble near the heated wall. *Journal of Thermal Science*. 2013;22(4):352-358. DOI: 10.1007/s11630-013-0635-9
- [18] Leighton TG, Cox BT, Phelps AD. The Rayleigh-like collapse of a conical bubble. *Journal of the Acoustical Society of America*. 2000;107(1):130-142. DOI: 10.1121/1.428296
- [19] Blake JR, Gibson DC. Cavitation bubbles near boundaries. *Annual Review of Fluid Mechanics*. 1987;19(1):99-123. DOI: 10.1146/annurev.fl.19.010187.000531
- [20] Ohl CD, Arora M, Ikink R, Jong ND, et al. Sonoporation from jetting cavitation bubbles. *Biophysical Journal*. 2006;91(11):4285-4295. DOI: 10.1529/biophysj.105.075366
- [21] Tzanakis I, Hadfield M, Henshaw I. Observations of acoustically generated cavitation bubbles within typical fluids applied to a scroll expander lubrication system. *Experimental Thermal and Fluid Science*. 2011;35(8):1544-1554. DOI: 10.1016/j.expthermflusci.2011.07.005
- [22] Plesset MS, Prosperetti A. Bubble dynamics and cavitation. *Annual Review of Fluid Mechanics*. 1977;9(1):145-185. DOI: 10.1146/annurev.fl.09.010177.001045
- [23] Hegedűs F, Klapcsik K. The effect of high viscosity on the collapse-like chaotic and regular periodic oscillations of a harmonically excited gas bubble. *Ultrasonics Sonochemistry*. 2015;27:153. DOI: 10.1016/j.ultsonch.2015.05.010
- [24] Chen H, Li J, Chen D, Wang J. Damages on steel surface at the incubation stage of the vibration cavitation erosion in water. *Wear*. 2008;265(5-6):692-698. DOI: 10.1016/j.wear.2007.12.011
- [25] Chen X, Yan J, Gao F, et al. Interaction behaviors at the interface between liquid Al-Si and solid Ti-6Al-4V in ultrasonic-assisted brazing in air. *Ultrasonics Sonochemistry*. 2013;20(1):144-154. DOI: 10.1016/j.ultsonch.2012.06.011

